7-2018

Primitive substitution tilings with rotational symmetries

April Lynne D. Say-Awen

Ma. Louise Antonette N. De Las Peñas
Ateneo de Manila University, mdelaspenas@ateneo.edu

Dirk Frettlöh
Universitat Bielefeld

Recommended Citation
Say-awen, A. L. D., De Las Peñas, M. L. A. N., & Frettlöh, D. (2018). Primitive substitution tilings with rotational symmetries. Acta Crystallographica Section A: Foundations and Advances, 74(4), 388-398.

FOUNDATIONS
ADVANCES

ISSN: 2053-2733
journals.iucr.org/a

Primitive substitution tilings with rotational symmetries

April Lynne D. Say-awen, Ma. Louise Antonette N. De Las Peñas and Dirk Frettlöh

Acta Cryst. (2018). A**74**, 388–398

Acta Cryst A
FOUNDATIONS
ADVANCES

ISSN 2053-2733

Received 9 January 2018
Accepted 2 May 2018

Edited by J.-G. Eon, Universidade Federal do Rio de Janeiro, Brazil

Keywords: symmetry order; aperiodic tilings; substitution tilings; rotation-invariant tilings; dense tile orientations.

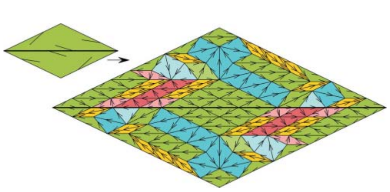

Primitive substitution tilings with rotational symmetries

April Lynne D. Say-awen,[a,b,c] Ma. Louise Antonette N. De Las Peñas[b]* and Dirk Frettlöh[d]

[a]Mathematics and Statistics Department, De La Salle University, Malate, Manila, 1004, Philippines, [b]Department of Mathematics, Ateneo de Manila University, Loyola Heights, Quezon City, 1108, Philippines, [c]CSCS Graduate Studies, De La Salle University – Dasmariñas, Dasmariñas, Cavite 4114, Philippines, and [d]Faculty of Technology, Bielefeld University, Postfach 100131, Bielefeld, 33501, Germany. *Correspondence e-mail: mdelaspenas@ateneo.edu

This work introduces the idea of symmetry order, which describes the rotational symmetry types of tilings in the hull of a given substitution. Definitions are given of the substitutions σ_6 and σ_7 which give rise to aperiodic primitive substitution tilings with dense tile orientations and which are invariant under six- and sevenfold rotations, respectively; the derivation of the symmetry orders of their hulls is also presented.

1. Introduction

Aperiodic substitution tilings have been a focus of study not only for their interesting algebraic, geometric and dynamical properties, but also because they are seen as potential structure models for quasicrystals, materials discovered in the early 1980s. See Baake & Grimm (2013), Frettlöh (2017), Kari & Rissanen (2016), Frank *et al.* (2016) and references therein. Understanding the properties of these tilings may lead to a better characterization of the structures they represent. One of the distinctive qualities of an aperiodic planar substitution tiling is n-fold rotational symmetry. It is an invariant of the tiling and its corresponding substitution tiling space. Moreover, it can differentiate a non-periodic tiling from a periodic one, since periodic tilings can only have two-, three-, four- or sixfold rotational symmetries (Baake & Grimm, 2013).

Most of the well known substitution tilings have the characteristic that their tiles occur in finitely many different orientations. An example of this tiling is the Penrose dart and kite tiling (Penrose, 1978). Its tiles occur in ten different orientations. There are also substitution tilings with tiles that occur in infinitely many orientations, such as the pinwheel tiling (Radin, 1994). More precisely, the pinwheel tiling has *dense tile orientations* (DTO), that is, the orientations of its tiles are dense in a unit circle. These characteristics of the pinwheel tilings give rise to interesting diffraction properties closely related to amorphous systems or regular crystals investigated by powder diffraction [see *e.g.* Grimm & Deng (2011), Baake *et al.* (2007*a*,*b*) and Moody *et al.* (2006) for more details]. Apart from DTO, the pinwheel tiling has the property that its hull contains six non-congruent tilings invariant under twofold rotation. This information is relevant in the computation of the cohomology of its tiling space (Barge *et al.*, 2010). In this light, Savinien posed the question of whether there are other primitive tilings with DTO invariant under n-fold rotation (Savinien & Frettlöh, 2013).

In this article we present substitutions σ_6 and σ_7 which generate primitive substitution tilings with DTO and which are invariant under n-fold rotation, $n \in \{6, 7\}$, respectively. The problem of finding the orders of rotational symmetries in the hull of a substitution is addressed, including the determination of all non-congruent tilings in the hull that are invariant under r-fold rotation, for some r up to translations or rigid motions. We note that the substitution σ_6 was first introduced by Frettlöh *et al.* (2017), where it was shown to have DTO and every tiling in its hull has finite local complexity (FLC) with respect to rigid motions, its hull containing two tilings invariant under sixfold rotation.

In this article, σ_6 is presented alongside σ_7, in the discussion of symmetry order and particularly to illustrate the notion of finding all the non-congruent tilings in a hull of a rotation-invariant substitution tiling.

2. General notions and definitions

A *tile* is a nonempty compact set $T \subset \mathbb{R}^2$ which is the closure of its interior. The *support* of a set of tiles is the union of its tiles. A *tiling* of $\mathbb{R}^2$ is a collection of tiles $\mathcal{T} = \{T_i \mid i \in \mathbb{N}\}$ such that its support is $\mathbb{R}^2$ and the intersection of the interiors of two distinct tiles T_i and T_j is empty. A finite set $\mathcal{P} \subset \mathcal{T}$ of tiles is called a *patch* of $\mathcal{T}$. Examples of patches of tilings are vertex stars and edge types. A *vertex star* of $\mathcal{T}$ is a patch of all tiles intersecting some vertex in $\mathcal{T}$. An *edge type* of $\mathcal{T}$ is a patch consisting of two tiles that intersect along an edge. Two tiles or patches of $\mathcal{T}$ are *equivalent* if the tiles or patches, respectively, can be made to coincide with each other by an isometry in $\mathbb{R}^2$.

For each tiling $\mathcal{T}$ of $\mathbb{R}^2$, we can form a new tiling by translating every tile of $\mathcal{T}$ by a nonzero $\mathbf{t} \in \mathbb{R}^2$. This tiling is referred to as the *translate* of $\mathcal{T}$ by $\mathbf{t}$, denoted by $\mathcal{T} + \mathbf{t} = \{T + \mathbf{t} \mid T \in \mathcal{T}\}$. A tiling $\mathcal{T}$ of $\mathbb{R}^2$ is called *periodic* if there is a nonzero vector $\mathbf{t} \in \mathbb{R}^2$ such that $\mathcal{T} + \mathbf{t} = \mathcal{T}$; otherwise, $\mathcal{T}$ is *non-periodic*. A tiling $\mathcal{T}$ of $\mathbb{R}^2$ is *aperiodic* if it is non-periodic and each tiling in its hull $\mathbb{X}_{\mathcal{T}}$ is non-periodic. The *hull* $\mathbb{X}_{\mathcal{T}}$ of a tiling $\mathcal{T}$ of $\mathbb{R}^2$ is the closure of the set $\{g\mathcal{T} \mid g \in G\}$ in the local topology where G is the group of all translations in $\mathbb{R}^2$ or the group of all rigid motions in $\mathbb{R}^2$. Closure is taken with respect to the local topology, which can be defined *via* a metric. In this metric two tilings are ε-close if they agree on a ball of radius $1/\varepsilon$ around the origin, after a small translation or rigid motion.

One way to generate aperiodic tilings is to use a substitution. Let $\mathcal{F} := \{T_1, T_2, \ldots, T_m\}$ be a finite set of tiles and $\lambda > 1$ a real number. For each $1 \le i \le m$, let $\lambda T_i = \bigcup_{j=1}^{n(i)} T_{i_j}$ such that each T_{i_j} is equivalent to a tile in $\mathcal{F}$ and the tiles $T_{i_1}, T_{i_2}, \ldots, T_{i_{n(i)}}$ have pairwise disjoint interiors. Let $\mathcal{S}$ be the collection of all sets of tiles equivalent to tiles in $\mathcal{F}$. We define σ to be the mapping $\sigma: \mathcal{F} \to \mathcal{S}$ given by $\sigma(T_i) = \{T_{i_1}, T_{i_2}, \ldots, T_{i_{n(i)}}\}$, $1 \le i \le m$. The mapping σ is called a *substitution* with *prototiles* $T_1, T_2, \ldots, T_m$ and *substitution factor* λ.

Throughout this article, we use $\mathfrak{R}_\theta$ to denote a rotation through an angle $\theta \in [0, 2\pi)$ about the origin and $\mathfrak{S}_l$ to denote a reflection across a line l passing through the origin. If T is an equivalent copy of a prototile T_i of a substitution σ, then T can be written either as (i) $T = \mathfrak{R}_\theta T_i + \mathbf{t}$ or (ii) $T = \mathfrak{R}_\theta \mathfrak{S}_l T_i + \mathbf{t}$, where $\mathbf{t} \in \mathbb{R}^2$. In the former case, we consider T as a *rotated copy* of T_i and in the latter case we consider T as a *reflected copy* of T_i. For later purposes, we call the angle θ an *orientation angle* of T. Now, by setting $\sigma(T) = \sigma(\mathfrak{R}_\theta T_i + \mathbf{t}) = \mathfrak{R}_\theta \sigma(T_i) + \lambda\mathbf{t}$ or $\sigma(T) = \sigma(\mathfrak{R}_\theta \mathfrak{S}_l T_i + \mathbf{t}) = \mathfrak{R}_\theta \mathfrak{S}_l \sigma(T_i) + \lambda\mathbf{t}$, σ extends naturally to any copy of a prototile. Given $\mathcal{A} \in \mathcal{S}$, σ extends to any set in $\mathcal{S}$ by $\sigma(\mathcal{A}) = \{\sigma(T) \mid T \in \mathcal{A}\}$. In particular, σ can be applied on T_i k times to obtain the *k-order supertile* $\sigma^k(T_i)$ of T_i.

As an example, let T be a right triangle whose legs measure 1 and 2. Inflate T by a factor of $\sqrt{5}$, then dissect $\sqrt{5}T$ into five equivalent copies of T (see Fig. 1). We define a mapping σ_p on T such that $\sigma_p(T)$ is the set containing the five right triangles whose union is $\sqrt{5}T$. The mapping σ_p is known as the *pinwheel* substitution (Radin, 1994) with one prototile and substitution factor $\sqrt{5}$. The first three supertiles of the pinwheel prototile are shown in Fig. 2. Applying the substitution σ_p repeatedly to T gives rise to a tiling $\mathcal{T}^*$ (pinwheel tiling) of $\mathbb{R}^2$. The hull of this tiling $\mathcal{T}^*$ is the set of all tilings containing the same patches as $\mathcal{T}^*$ (Baake & Grimm, 2013).

Remark 1. Note that, in certain situations, it is helpful to distinguish T_i and its reflected copy as two non-equivalent prototiles.

A substitution σ can produce a tiling by iteratively applying σ on a prototile, called a substitution tiling with respect to σ. In general, a tiling $\mathcal{T}$ is called a *substitution tiling* with respect to the substitution σ if for each patch $\mathcal{P} \subset \mathcal{T}$ there is a prototile T_i and $k \in \mathbb{N}$ such that an equivalent copy of $\mathcal{P}$ is contained in $\sigma^k(T_i)$. Substitutions on tilings are also referred to as inflations.

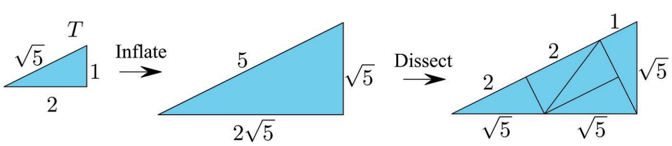

Figure 1
The pinwheel substitution.

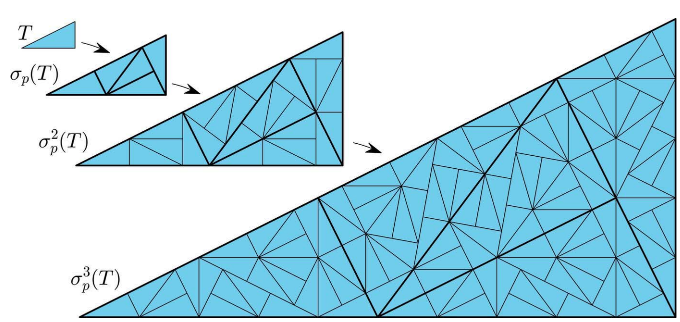

Figure 2
The k-order supertiles of the pinwheel prototile, $k = 1, 2, 3$.

One of the interesting properties of a substitution is primitivity. A substitution is *primitive* if there is a $k \in \mathbb{N}$ such that each k-order supertile contains equivalent copies of all prototiles. A substitution tiling $\mathcal{T}$ with respect to a primitive substitution is called a *primitive* substitution tiling. The set of all substitution tilings with respect to the substitution σ is called the *hull* of σ, denoted by $\mathbb{X}_\sigma$. If σ is primitive, it is well known that for every $\mathcal{T} \in \mathbb{X}_\sigma$, $\mathbb{X}_\mathcal{T} = \mathbb{X}_\sigma$.

In this work, we will consider primitive aperiodic substitution tilings that are repetitive and have finite local complexity (with respect to rigid motions) and DTO. A tiling $\mathcal{T}$ has *finite local complexity* (FLC) if for a fixed $r > 0$ there are only finitely many non-equivalent patches in $\mathcal{T}$ fitting into a ball B_r of radius r (called *r-patches*), while a tiling $\mathcal{T}$ is *repetitive* if for every $r > 0$ there exists $R = R(r) > 0$ such that every R-patch of $\mathcal{T}$ contains an equivalent copy of every r-patch of $\mathcal{T}$.

A tiling $\mathcal{T}$ has DTO if the set of orientation angles of the tiles in $\mathcal{T}$ is dense in $[0, 2\pi)$ (Frettlöh, 2008). Now, if a primitive substitution tiling has DTO then its hull with respect to the group of all translations and its hull with respect to the group of all rigid motions coincide (Frettlöh & Richard, 2014). So in our case it does not matter which we choose. One of the first known examples of primitive substitution tilings with DTO are the tilings in $\mathbb{X}_{\sigma_p}$.

The hull of the pinwheel tiling has the property that it contains six non-congruent tilings invariant under twofold rotation (Frettlöh *et al.*, 2014; Baake *et al.*, 2007*a*). A substitution tiling that is *invariant under n-fold rotation* contains bounded n-fold rotation-invariant patches of arbitrary radius centred on its centre of n-fold rotation (Maloney, 2015).

A patch $\mathcal{P}$ that is invariant under n-fold rotation may serve as a seed for n-fold rotation-invariant tiling in the following manner. Suppose $\mathcal{P}$ and its supertiles (arising from a substitution σ) are invariant under n-fold rotation about the origin, and suppose there exists $q \in \mathbb{N}$ such that $(\mathfrak{R}_\theta\sigma)^q(\mathcal{P})$ contains $\mathcal{P}$ in its centre for some $\theta \in [0, 2\pi)$. Then we obtain a nested sequence $((\mathfrak{R}_\theta\sigma)^{qk}(\mathcal{P}))_{k\in\mathbb{N}}$ that converges to a tiling $\mathcal{T}$ invariant under n-fold rotation that is a fixed point of $(\mathfrak{R}_\theta\sigma)^q$. In this case $\mathcal{P}$ is a *seed* for $\mathcal{T}$.

As an example, consider the patch $\mathcal{V}$ of a pinwheel tiling that is invariant under twofold rotation (see Fig. 3). Let $\mathcal{V}$ be centred at the origin. Observe that $\sigma_p^2(\mathcal{V})$ contains $\mathcal{V}$ in its centre. Thus $(\sigma_p^{2k}(\mathcal{P}))_{k\in\mathbb{N}}$ converges to a tiling invariant under twofold rotation that is a fixed point of σ_p^2. In this example, $\mathfrak{R}_\theta$ is the trivial rotation.

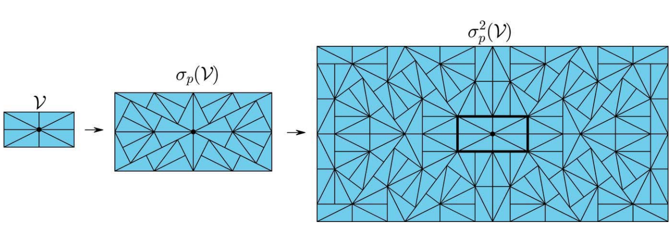

Figure 3
$\sigma_p^2(\mathcal{V})$ contains $\mathcal{V}$ in its centre.

3. Substitution tilings with DTO invariant under six- and sevenfold rotations

To arrive at a tiling invariant under sixfold or sevenfold rotation, we use the method from Say-awen (2016) and Frettlöh *et al.* (2017) given as follows.

(i) Choose a first prototile $T_1^{(n)}$ to be a regular n-gon of unit edge length.

(ii) The substitution σ_n of $T_1^{(n)}$ is given by a regular n-gon with edge length λ_n, which is dissected to contain an equivalent copy of $T_1^{(n)}$ in its centre and n equivalent copies of a triangle $T_2^{(n)}$ along its edges, and if $n \geq 5$, into several parallelograms (Fig. 4). Moreover, the resulting dissection must be invariant under n-fold rotation. The triangle $T_2^{(n)}$ is a prototile which has interior angle

$$\theta_n = \begin{cases} \frac{(n-1)\pi}{n} & \text{if } n \text{ is odd} \\ \frac{(n-2)\pi}{n} & \text{if } n \text{ is even,} \end{cases}$$

where the two edges forming this angle have lengths 1 and 2, respectively. By straightforward calculations using, for example, the cosine law, the length λ_n of the longest edge of $T_2^{(n)}$ is

$$\lambda_n = \begin{cases} \sqrt{5 + 4\cos\left(\frac{\pi}{n}\right)} & \text{if } n \text{ is odd} \\ \sqrt{5 + 4\cos\left(\frac{2\pi}{n}\right)} & \text{if } n \text{ is even.} \end{cases}$$

Thus, the substitution factor equals λ_n.

(iii) Continue defining the substitution σ_n, $n \geq 5$, to $T_1^{(n)}$ by dissecting the parallelograms into triangles, giving rise to additional prototiles $T_j^{(n)}$ for some $j > 2$ (see Fig. 5 for $n = 6$).

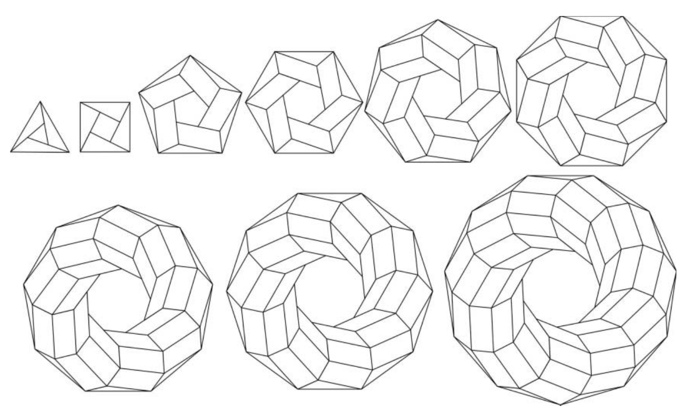

Figure 4
Dissection of the regular n-gon with length λ_n for $3 \leq n \leq 11$.

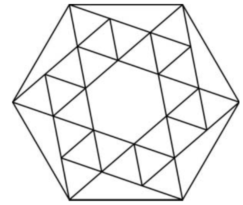

Figure 5
A dissection of the parallelograms for $n = 6$.

(iv) The substitution σ_n is defined for other prototiles $T_j^{(n)}$, $2 \le j \le q$, by inflating $T_j^{(n)}$ by a factor of λ_n and dissecting $\lambda_n T_j^{(n)}$ into tiles such that each tile is equivalent to a prototile. The polygons in the dissection of $\lambda_n T_j^{(n)}$ form the image $\sigma_n(T_j^{(n)})$ of $T_j^{(n)}$ under σ_n. It may happen that $\lambda_n T_j^{(n)}$ cannot be dissected using only the existing prototiles, and it is necessary to introduce new prototiles, which are triangles $T_{q+1}^{(n)}, T_{q+2}^{(n)}, \ldots, T_s^{(n)}$. The substitution of the additional prototiles will be constructed the same way.

For $n = 6$, the substitution factor is $\lambda_6 = \sqrt{7}$. The substitution σ_6 is defined using four prototiles $T_1^{(6)}$, $T_2^{(6)}$, $T_3^{(6)}$ and $T_4^{(6)}$ (Fig. 6). The parallelograms are dissected into equivalent copies of $T_3^{(6)}$. It can be checked that $\sqrt{7}T_3^{(6)}$ can be dissected into equivalent copies of $T_2^{(6)}$ and $T_3^{(6)}$, but the prototile $T_4^{(6)}$ is introduced in this substitution to ensure primitivity.

For $n = 7$, the substitution factor is $\lambda_7 = [5 + 4\cos(\pi/7)]^{1/2}$ and the prototiles are given in Figs. 7 and 8. Here, the edges are equipped with half-arrows to indicate their orientations. Edge orientations are helpful to ensure FLC. We note that the orientation of a symmetric tile is apparent from the half-arrows on its edges. For example, the two tiles marked by dots in $\sigma_7(T_1^{(7)})$ in Fig. 8 can be identified as reflected images of each other using the half-arrows on their edges as a guide.

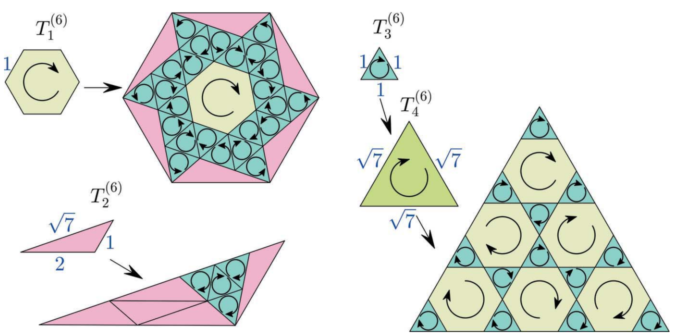

Figure 6
The substitution σ_6. The circular arrows indicate the orientations of symmetric tiles.

Remark 2. By construction, σ_n, $n \in \{6, 7\}$, preserves the rotational symmetry of each prototile. For instance, $T_3^{(6)}$ is invariant under threefold rotation, as well as its supertiles $\sigma_6^k(T_3^{(6)})$ for all $k \in \mathbb{N}$.

In the following theorem, we show the existence of tilings $\mathcal{T}_n$ invariant under n-fold rotation arising from σ_n, $n \in \{6, 7\}$.

Theorem 3. There exists a substitution tiling $\mathcal{T}_n$ with respect to σ_n that is invariant under n-fold rotation, $n \in \{6, 7\}$.

Proof. Consider σ_n, $n \in \{6, 7\}$, with corresponding prototiles $T_1^{(n)}$ and $T_2^{(n)}$. Let $\mathfrak{R}_{\alpha_n}$ be the rotation about the origin through α_n, where α_n is the smallest interior angle of $T_2^{(n)}$. Moreover, let $T_1^{(n)}$ be centred at the origin. Then $\mathfrak{R}_{\alpha_n}(\sigma_n(T_1^{(n)}))$ contains $T_1^{(n)}$ in its centre. Consequently, $(\mathfrak{R}_{\alpha_n}\sigma_n)^k(T_1^{(n)})$ contains $(\mathfrak{R}_{\alpha_n}\sigma_n)^{k-1}(T_1^{(n)})$ in its centre (see Fig. 9 for $k = 1, 2$ and $n = 6$). Hence $((\mathfrak{R}_{\alpha_n}\sigma_n)^k(T_1^{(n)}))_{k\in\mathbb{N}}$ is a nested sequence that converges to a tiling $\mathcal{T}_n$ which is invariant under n-fold rotation. The n-fold rotation-invariant prototile $T_1^{(n)}$ serves as a seed for the tiling $\mathcal{T}_n$, which is also a fixed point of $\mathfrak{R}_{\alpha_n}\sigma_n$. □

To show the occurrence of DTO in a tiling in the hull, we employ the following result. The ('only if') direction is from Frettlöh (2008). A stronger version of the ('if') direction appears in Frettlöh (2008) and Radin (1994, 1995); that is, the orientation angles of the tiles are not only dense on the circle but also uniformly distributed in $[0, 2\pi)$. In the theorem below, an angle $\alpha \in [0, 2\pi)$ is *irrational* if $\alpha \notin \pi\mathbb{Q}$.

Theorem 4. Let σ be a primitive substitution in $\mathbb{R}^2$ with prototiles $T_1, T_2, \ldots, T_m$. Any substitution tiling in $\mathbb{X}_\sigma$ has DTO if and only if there are $k \in \mathbb{N}$ and $i \in \{1, 2, \ldots, m\}$ such that $\sigma^k(T_i)$ contains two equivalent tiles that are rotated against each other by some irrational angle.

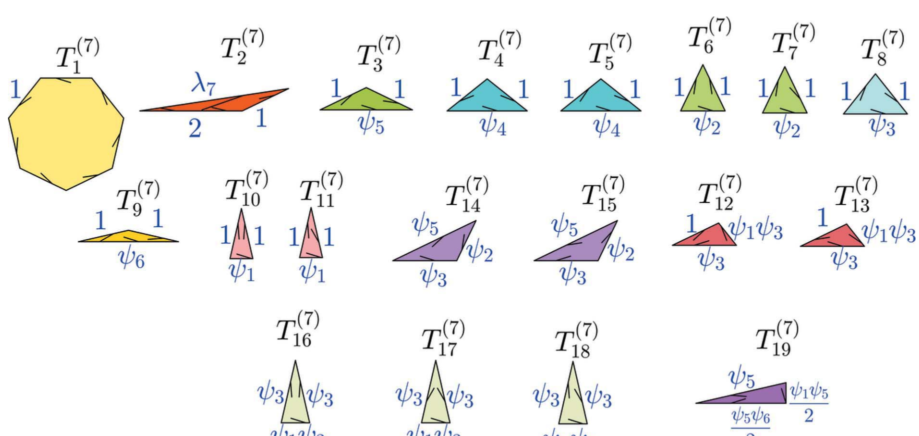

Figure 7
The first 19 prototiles of σ_7. The edge lengths of each tile are given, where $\psi_i = 2\sin(\pi i/14)$, $i \in \{1, 2, 3, 4, 5, 6\}$.

The following result is from Frettlöh *et al.* (2017) and is probably older, which alongside theorem 4 facilitates proving DTO for the tilings in the hull of σ_n.

Theorem 5. Let P be a parallelogram with edge lengths 1 and 2 and interior angles $2\pi/r$ and $[(r-2)\pi]/r$, $r \geq 3$ (see Fig. 10). Then the angles between the longer diagonal of P and the edges of P are irrational.

Using the above results, we now prove the following.

Theorem 6. Each tiling $\mathcal{T} \in \mathbb{X}_{\sigma_n}$, $n \in \{6, 7\}$, has DTO.

Proof. Consider the tiles T and T' lying along the boundaries of rotated copies of $\sigma_n(T_1^{(n)})$ and $\sigma_n^3(T_1^{(n)})$ as shown in Figs. 11 and 12, respectively, for $n = 6, 7$. As described in theorem 3, the boundaries are rotated against each other by $2\alpha_n$, where α_n is the smallest interior angle of $T_2^{(n)}$. Thus the two tiles are rotated against each other by $2\alpha_n$.

Now, the prototiles $T_2^{(6)}$ and $T_2^{(7)}$ have interior angles $2\pi/3$ and $6\pi/7$, respectively, where the edges forming each of these angles have lengths 1 and 2. It follows that the triangle $T_2^{(n)}$, $n \in \{6, 7\}$, is congruent to the triangle with vertices 0, 2, z in Fig. 10 with $r = 6$ if $n = 6$ and $r = 14$ if $n = 7$. So α_n is irrational by theorem 5. Consequently, $2\alpha_n$ is irrational. Thus $\sigma_n^3(T_1^{(n)})$ contains two equivalent tiles that are rotated against each other by an irrational angle. Therefore, each tiling in the hull of σ_n has DTO by theorem 4. □

Next, we will show in theorem 8 that each tiling in $\mathbb{X}_{\sigma_n}$, $n \in \{6, 7\}$, has FLC. Note that since FLC and primitivity imply repetitivity [see Frettlöh & Richard (2014) for a proof], the tilings are repetitive as well. In Frettlöh & Richard (2014), the following lemma was also pointed out.

Lemma 7. A substitution tiling $\mathcal{T}$ with respect to a substitution σ with a finite prototile set consisting of polygons satisfying the condition that the tiles in $\sigma^k(T_i)$ meet full-edge to full-edge for all $k \in \mathbb{N}$ and for all prototiles T_i of σ implies $\mathcal{T} \in \mathbb{X}_\sigma$ has FLC.

Theorem 8. Each tiling $\mathcal{T} \in \mathbb{X}_{\sigma_n}$, $n \in \{6, 7\}$, has FLC.

Proof. For each $n \in \{6, 7\}$, the prototile set of σ_n is finite and the prototiles are all polygons. To ensure FLC, the substitutions are defined such that tiles in each supertile of a prototile meet full-edge to full-edge. In the construction process an

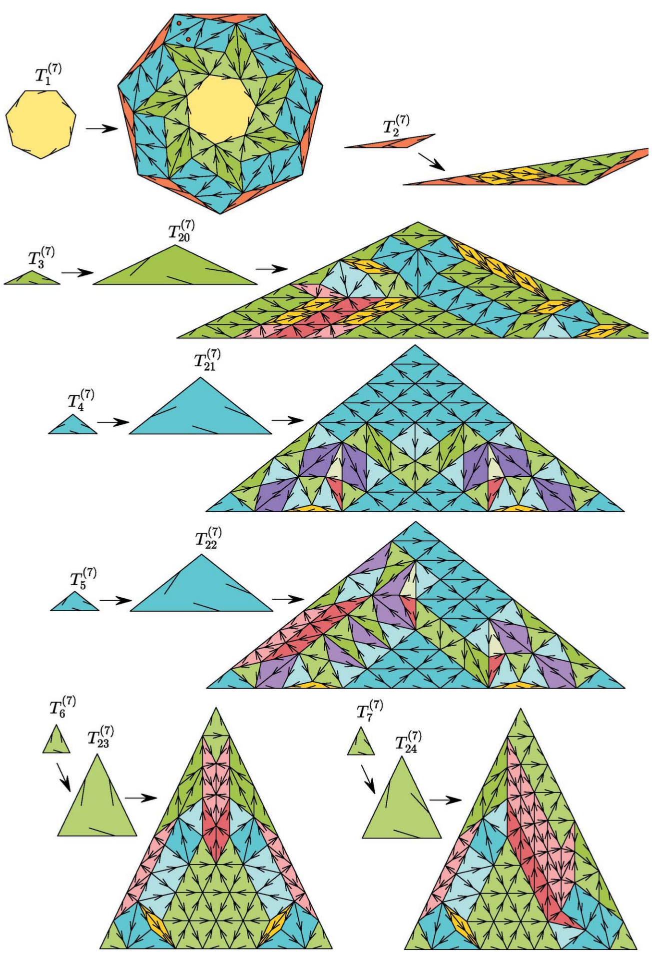

(*a*)

Figure 8
The substitution σ_7. The prototiles $T_j^{(7)}, j \in \{20, 21, \ldots, 36\}$, are shown.

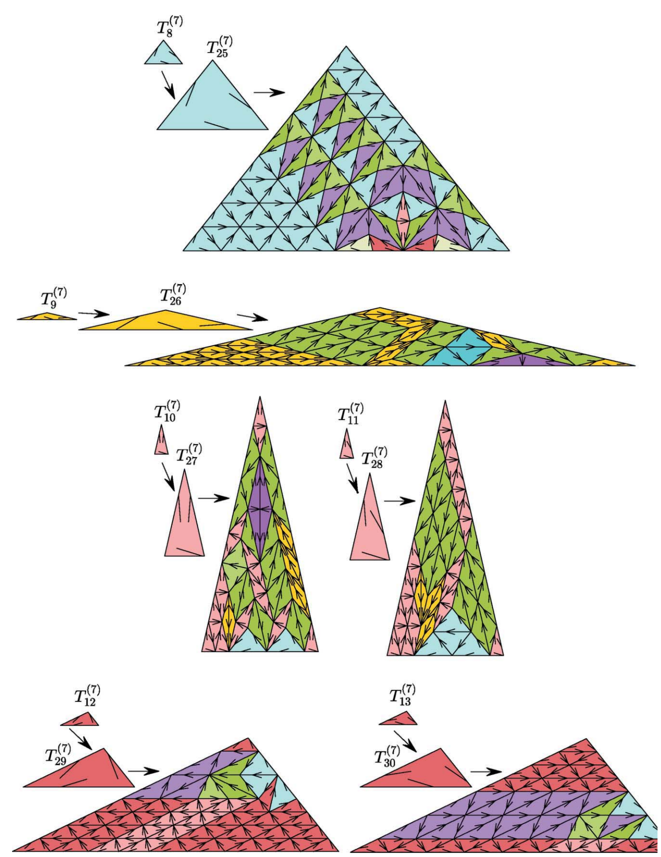

(*b*)

Figure 8 (continued)
The substitution σ_7. The prototiles $T_j^{(7)}, j \in \{20, 21, \ldots, 36\}$, are shown.

additional vertex (pseudo-vertex) is introduced at the midpoint of the edge of length 2 in $T_2^{(n)}$, $n \in \{6, 7\}$. Taking into account this pseudo-vertex, the tiles in each 1-order supertile meet full-edge to full-edge. For instance, in Fig. 13, if a pseudo-vertex (red dot) is introduced, the pink and blue tiles meet full-edge to full-edge. Moreover, inflated edges by λ_n, $n \in \{6, 7\}$, of the same length are dissected in the same manner. For instance, the image of each edge of length 1 for $n = 6$ is an edge of length $\sqrt{7}$, and the image of each edge of length $\sqrt{7}$ is a composition of 7 edges of length 1 (Fig. 6). For $n = 6$, this guarantees that the tiles in any supertile meet full-edge to full-edge. Consider any two tiles T and T' in a 1-order supertile $\sigma_6(T_i)$ meeting at an edge. Observe that the length of this edge is 1. Hence, $\sigma_6(T)$ and $\sigma_6(T')$ meet at an edge of length $\sqrt{7}$ in ${\sigma_6}^2(T_i)$. As a result, ${\sigma_6}^2(T)$ and ${\sigma_6}^2(T')$ meet at a super-edge of length 7. Since a super-edge of length 7 is a composition of 7 edges of length 1, then tiles meet at the super-edge full-edge to full-edge. The same analysis applies to any pair of two tiles meeting at the super-edge.

For $n = 7$, additional prototiles are introduced. It is possible to define σ_7 using only 20 prototiles: $T_j^{(7)}$, $j \in \{1, 2, 3, 5, 6, 8, 9, 12, 14, 16, 19, 20, 22, 23, 25, 26, 29, 31, 33, 36\}$. But to ensure FLC, the substitution is defined using 36 prototiles. In the case where two coincident edges have opposite orientations, the composition of their super-edges is such that it is mirror

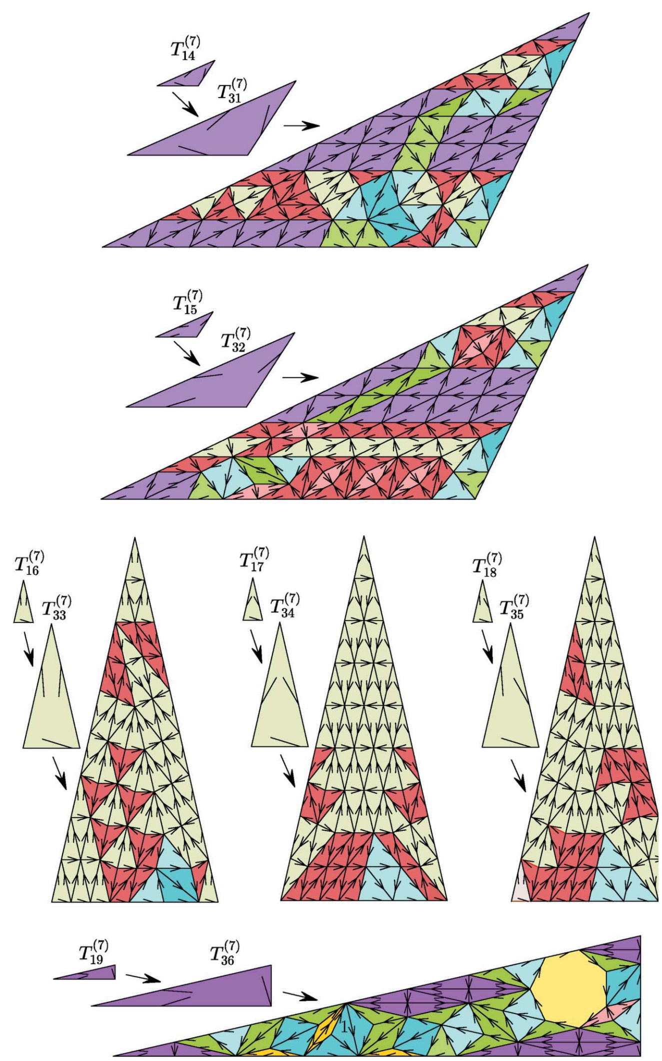

(c)

Figure 8 (continued)
The substitution σ_7. The prototiles $T_j^{(7)}$, $j \in \{20, 21, \ldots, 36\}$, are shown.

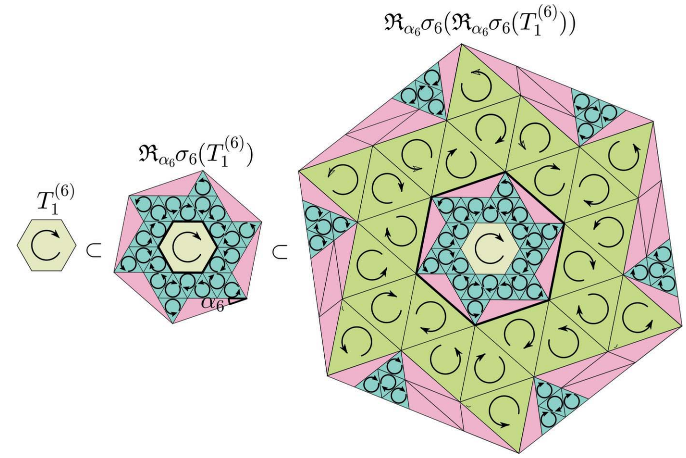

Figure 9
The first three terms of the nested sequence $((\mathfrak{R}_{\alpha_6}\sigma_6)^k(T_1^{(6)}))_{k\in\mathbb{N}}$.

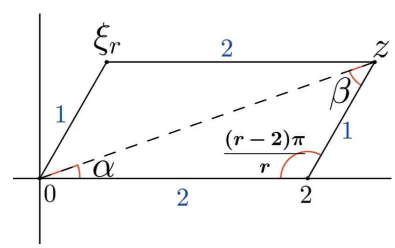

Figure 10
The parallelogram P.

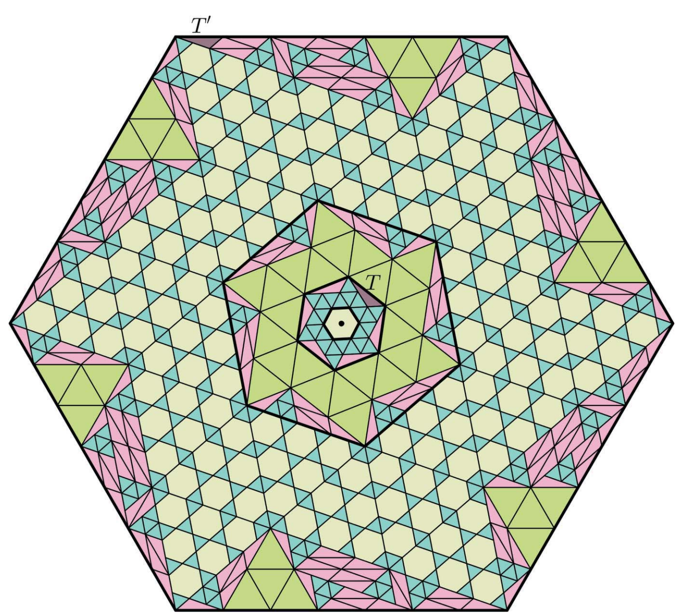

Figure 11
Tiles T and T' in $\sigma_6^3(T_1^{(6)})$ are rotated against each other by $2\alpha_6$.

symmetric about its midpoint. For example, a super-edge of length $\lambda_7\psi_5 = 4 + 5\psi_5 + 2\psi_3$ has the composition $\psi_5 - 1 - \psi_3 - 1 - \psi_5 - \psi_5 - \psi_5 - 1 - \psi_3 - 1 - \psi_5$. An example of such super-edge is the longest super-edge of $\sigma_7(T_{20}^{(7)})$ as shown in Fig. 14. This ensures that the tiles in any supertile meet full-edge to full-edge (see Fig. 15 for an illustration).

By the above considerations, a substitution tiling with respect to σ_n, $n \in \{6, 7\}$, will satisfy the condition that the tiles in $\sigma_n^k(T_i)$ meet full-edge to full-edge for all $k \in \mathbb{N}$ and for all protottiles T_i. Thus, each tiling $\mathcal{T} \in \mathbb{X}_{\sigma_n}$ has FLC by lemma 7. □

To prove aperiodicity of a tiling in the hull, we need the following results. Theorem 9 is from Grünbaum & Shephard (1986) and theorem 10 is from Baake & Grimm (2013).

Theorem 9. A substitution tiling with respect to a substitution is non-periodic if in this tiling the 1-order supertiles can be identified in a unique way.

Theorem 10. A repetitive tiling in $\mathbb{R}^2$ that is non-periodic is aperiodic.

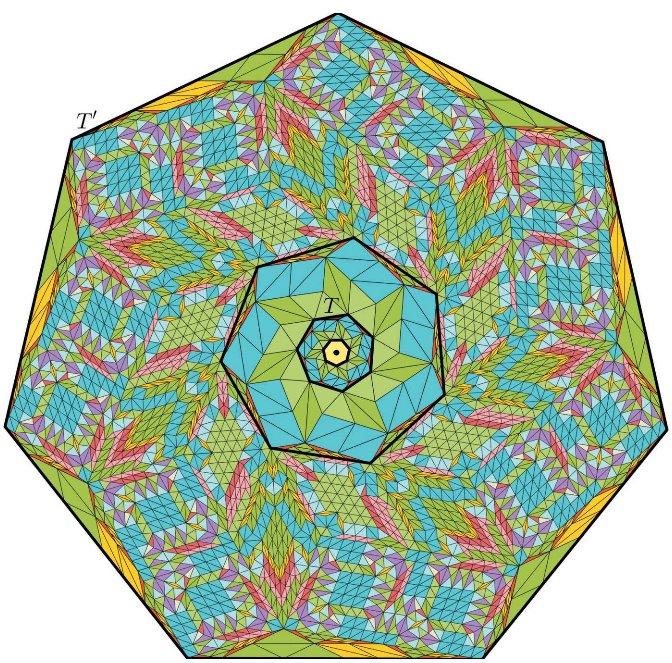

Figure 12
Tiles T and T' in $\sigma_7^3(T_1^{(7)})$ are rotated against each other by $2\alpha_7$.

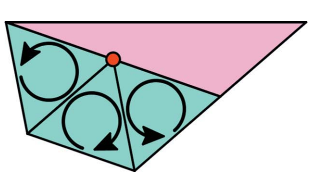

Figure 13
A patch of $\sigma_6(T_1^{(6)})$ is shown.

Theorem 11. Each tiling $\mathcal{T} \in \mathbb{X}_{\sigma_n}$, $n \in \{6, 7\}$, is aperiodic.

Proof. It can be shown that the 1-order supertiles of $\mathcal{T} \in \mathbb{X}_{\sigma_n}$, $n \in \{6, 7\}$, can be identified in a unique way. Hence $\mathcal{T}$ is non-periodic by theorem 9. Moreover, since $\mathcal{T}$ is also repetitive, $\mathcal{T}$ is aperiodic by theorem 10. □

4. Symmetry order

In this section we introduce the idea of symmetry order, which describes the rotational symmetry types of tilings in the hull of a given substitution. The *symmetry order* of the hull $\mathbb{X}_\sigma$ of a substitution σ is given by $(r_1, r_2, \ldots, r_q)$ such that $r_1 < r_2 < \ldots < r_q$ and each $r_i \in \mathbb{N}$ is the order of a rotational symmetry of some tiling $\mathcal{T} \in \mathbb{X}_\sigma$.

To determine the symmetry order of $\mathbb{X}_\sigma$, we look at finite (small as possible) patches arising from σ that are invariant under r-fold rotation which could serve as seeds for r-fold rotation-invariant tilings. In such a patch, a centre of rotational symmetry can be (*a*) the centre of a tile, (*b*) a vertex or (*c*) the midpoint of an edge of the tiling. The possibilities are prototiles, vertex stars or edge types of σ.

Theorem 12. The symmetry order of $\mathbb{X}_{\sigma_6}$ is (2, 3, 6). The symmetry order of $\mathbb{X}_{\sigma_7}$ is (2, 7).

Proof. The prototile $T_1^{(6)}$ is a seed for the tiling $\mathcal{T}_6 \in \mathbb{X}_{\sigma_6}$ invariant under sixfold rotation (Fig. 9). Similarly, if $T_3^{(6)}$ and $T_4^{(6)}$ are centred at the origin, then $\sigma_6^2(T_3^{(6)})$ and $\sigma_6^2(T_4^{(6)})$ contain

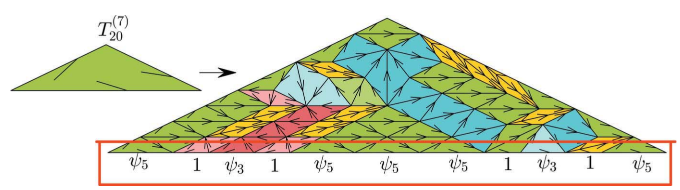

Figure 14
The composition of the longest super-edge of $\sigma_7(T_{20}^{(7)})$ is symmetric about its midpoint.

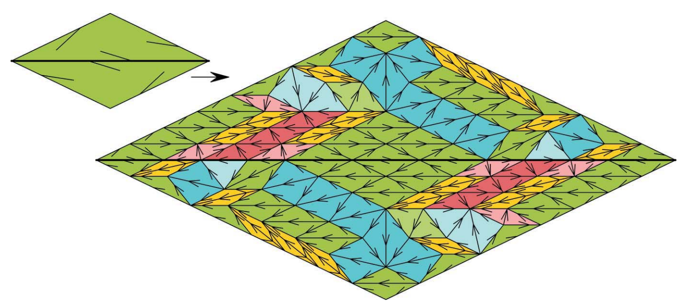

Figure 15
The tiles on the longest boundaries of the two supertiles meet full-edge to full-edge.

$T_3^{(6)}$ and $T_4^{(6)}$ in their centres, respectively (see Fig. 16). Hence $T_3^{(6)}$ and $T_4^{(6)}$ are seeds for tilings in $\mathbb{X}_{\sigma_6}$ invariant under threefold rotation. Now, examples of vertex stars that are invariant under twofold rotation are the patches $\mathcal{V}_{6,3}$ and $\mathcal{V}_{6,4}$ shown in Fig. 17. Let $\mathcal{V}_{6,3}$ and $\mathcal{V}_{6,4}$ be centred at the origin. As illustrated in Fig. 18, the centre of $\sigma_6(\mathcal{V}_{6,3})$ is $\mathcal{V}_{6,4}$ and the centre of $\sigma_6(\mathcal{V}_{6,4})$ is $\mathcal{V}_{6,3}$. It follows that $\sigma_6^2(\mathcal{V}_{6,3})$ and $\sigma_6^2(\mathcal{V}_{6,4})$ contain $\mathcal{V}_{6,3}$ and $\mathcal{V}_{6,4}$ in their centres, respectively. Thus $(\sigma_6^{2k}(\mathcal{V}_{6,3}))_{k\in\mathbb{N}}$ and $(\sigma_6^{2k}(\mathcal{V}_{6,4}))_{k\in\mathbb{N}}$ converge to two tilings in $\mathbb{X}_{\sigma_6}$ invariant under twofold rotation with seeds $\mathcal{V}_{6,3}$ and $\mathcal{V}_{6,4}$, respectively. Morever, we note that the order of a non-trivial rotational symmetry of an edge type is always 2. Therefore, since there are no other prototiles, vertex stars and edge types (see Fig. 17) that have rotational symmetries with orders aside from 2, 3 and 6, the symmetry order of $\mathbb{X}_{\sigma_6}$ is (2, 3, 6).

For $n = 7$, the prototile $T_1^{(7)}$ is a seed for the tiling $\mathcal{T}_7 \in \mathbb{X}_{\sigma_6}$ that is invariant under sevenfold rotation. From the prototile set (Fig. 7) of σ_7, $T_1^{(7)}$ is the only prototile that has rotational symmetry. In particular there are no prototiles invariant under two-, three-, four-, five- and sixfold rotation. Now, it can be checked that the highest order of a rotational symmetry of a vertex star is 2. Examples of such vertex stars are shown in Fig. 19. In particular, consider $\mathcal{W}_{2,1}$ and let it be centred at the origin. As shown in Fig. 20, $\sigma_7^2(\mathcal{W}_{2,1})$ contains $\mathcal{W}_{2,1}$ in its centre. Thus $(\sigma_7^{2k}(\mathcal{W}_{2,1}))_{k\in\mathbb{N}}$ converges to a tiling in $\mathbb{X}_{\sigma_7}$ invariant under twofold rotation whose seed is $\mathcal{W}_{2,1}$. Therefore, the symmetry order of $\mathbb{X}_{\sigma_7}$ is (2, 7). □

Remark 13. A (rotation) symmetric patch such as a prototile, vertex star or edge type may not always be a seed for a rotation-invariant tiling. This needs to be verified by studying how the patch behaves under the given substitution. For example, as described in Fig. 17, for $k \geq 2$ the central patch of $\sigma_6^k(\mathcal{V}_{6,1})$ is an equivalent copy of $\mathcal{V}_{6,3}$ or $\mathcal{V}_{6,4}$. This indicates that $\mathcal{V}_{6,1}$ is not a seed for a tiling in $\mathbb{X}_{\sigma_6}$.

Apart from the problem of finding the orders of rotational symmetries in the hull of a substitution, a question that comes to mind is how to determine the non-congruent tilings in the hull invariant under r-fold rotation for some r up to translations or rigid motions. We illustrate this idea for $\mathbb{X}_{\sigma_6}$ in Theorem 15.

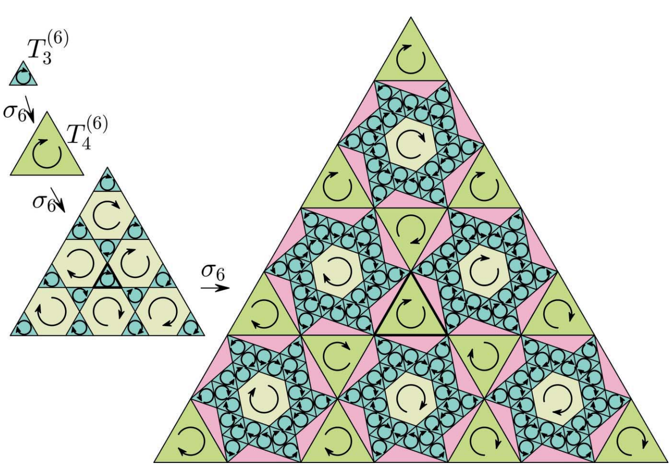

Figure 16
$\sigma_6^2(T_3^{(6)})$ and $\sigma_6^2(T_4^{(6)})$ contain $T_3^{(6)}$ and $T_4^{(6)}$, respectively, in their centres.

First, we give the following theorem, which is helpful in determining other possible seeds for rotation-invariant tilings in $\mathbb{X}_{\sigma_6}$. We also show in the theorem that a seed $\mathcal{P}$ for a tiling in the hull $\mathbb{X}_\sigma$ of a substitution σ and any reflected copy of $\mathcal{P}$ give rise to congruent tilings in $\mathbb{X}_\sigma$ up to rigid motions when $\mathcal{P}$ is mirror symmetric. A patch $\mathcal{P}$ in a tiling in $\mathbb{X}_\sigma$ is *mirror symmetric* if $\sigma^k(\mathcal{P})$ is invariant under a reflection for all k.

Theorem 14. Let σ be a primitive substitution. Suppose $\mathcal{P}$ is invariant under r-fold rotation and is a seed for a rotation-invariant tiling $\mathcal{T} \in \mathbb{X}_\sigma$. If $\mathcal{P}'$ is a patch of a supertile of σ and is a reflected copy of $\mathcal{P}$, then $\mathcal{P}'$ is a seed for a tiling $\mathcal{T}' \in \mathbb{X}_\sigma$, which is a reflected image of $\mathcal{T}$. In addition, if $\mathcal{P}$ is mirror symmetric, $\mathcal{P}$ and $\mathcal{P}'$ give rise to congruent tilings in $\mathbb{X}_\sigma$ up to rigid motions.

Proof. Suppose $\mathcal{P}$ is a seed for a tiling $\mathcal{T}$ in $\mathbb{X}_\sigma$ invariant under r-fold rotation. Then $\mathcal{P}$ is the centre of $\sigma^q(\mathcal{P})$ for some $q \in \mathbb{N}$ and $\mathcal{T}$ is the limit of the nested sequence $(\sigma^{kq}(\mathcal{P}))_{k\in\mathbb{N}}$. Let $\mathcal{P}'$ be a reflected copy of $\mathcal{P}$. Without loss of generality, let $\mathcal{P}' = \mathfrak{S}_{l_1}\mathcal{P}$ for some reflection $\mathfrak{S}_{l_1}$. Now, $\mathcal{P}' = \mathfrak{S}_{l_1}\mathcal{P}$ and $\mathcal{P} \subset \sigma^q(\mathcal{P})$ imply that $\mathcal{P}' = \mathfrak{S}_{l_1}\mathcal{P} \subset \mathfrak{S}_{l_1}\sigma^q(\mathcal{P}) = \sigma^q(\mathfrak{S}_{l_1}\mathcal{P}) = \sigma^q(\mathcal{P}')$ and $\sigma^q(\mathcal{P}')$ contains $\mathcal{P}'$ in its centre. Thus $\mathcal{P}'$ is a seed for a tiling $\mathcal{T}' \in \mathbb{X}_\sigma$ invariant under r-fold rotation that is the limit of the nested sequence $(\sigma^{kq}(\mathcal{P}'))_{k\in\mathbb{N}}$. Moreover, $\mathcal{T}'$ is a reflected image of $\mathcal{T}$ because $\mathfrak{S}_{l_1}\sigma^{kq}(\mathcal{P}) = \sigma^{kq}(\mathcal{P}')$ for all $k \in \mathbb{N}$.

Now suppose $\mathcal{P}$ is mirror symmetric. Without loss of generality, we let $\mathfrak{S}_{l_2}\sigma^{kq}(\mathcal{P}) = \sigma^{kq}(\mathcal{P})$ for some reflection $\mathfrak{S}_{l_2}$. Thus $(\sigma^{kq}(\mathcal{P}'))_{k\in\mathbb{N}} = (\mathfrak{S}_{l_1}\sigma^{kq}(\mathcal{P}))_{k\in\mathbb{N}} = (\mathfrak{S}_{l_1}\mathfrak{S}_{l_2}\sigma^{kq}(\mathcal{P}))_{k\in\mathbb{N}}$. Thus $\mathcal{P}$ and $\mathcal{P}'$ give rise to congruent tilings up to rigid motions. □

Theorem 15. There are 16 non-congruent rotation-invariant tilings in $\mathbb{X}_{\sigma_6}$ up to rigid motions: two tilings invariant under sixfold rotation, four tilings invariant under threefold rotation and ten tilings invariant under twofold rotation.

Proof. First, let us show that each patch (or isometric image) of a tiling in $\mathbb{X}_{\sigma_6}$ has a reflected copy in some supertile of σ_6. Let $\mathcal{P}$ be a patch of a tiling in $\mathbb{X}_{\sigma_6}$. Then there exists $k \in \mathbb{N}$ and a prototile $T_j^{(6)}$, $j \in \{1, 2, 3, 4\}$, such that $\sigma_6^k(T_j^{(6)})$ contains an equivalent copy of $\mathcal{P}$. Now, consider the prototile $T_3^{(6)}$. Because σ_6 is primitive, there exists $q \in \mathbb{N}$ such that $\sigma_6^q(T_3^{(6)})$ contains an equivalent copy of $T_j^{(6)}$. Thus $\sigma_6^{q+k}(T_3^{(6)})$ contains an equivalent copy of $\mathcal{P}$, say $\mathcal{P}'$. Now observe that $T_3^{(6)}$ has a reflected copy $T_3^{(6)'}$ that occurs in $\sigma_6(T_1^{(6)})$ (see Fig. 6). Thus, $\sigma_6^{q+k}(T_3^{(6)'})$ is a reflected copy of $\sigma_6^{q+k}(T_3^{(6)})$ and contains a reflected copy of $\mathcal{P}'$. Thus $\mathcal{P}$ (or isometric image) has a reflected copy in a supertile of σ_6.

We now determine non-trivial rotation-invariant tilings in $\mathbb{X}_{\sigma_6}$. We know that the prototile $T_1^{(6)}$ is a seed for the tiling $\mathcal{T}_6 \in \mathbb{X}_{\sigma_6}$ invariant under sixfold rotation. From the above result, a reflected copy $T_1^{(6)'}$ of $T_1^{(6)}$ occurs in a supertile of σ_6. By theorem 14, $T_1^{(6)'}$ is also a seed for a tiling in $\mathbb{X}_{\sigma_6}$ invariant under sixfold rotation. Note that $T_1^{(6)}$ is not mirror symmetric. Thus the tilings arising from $T_1^{(6)}$ and $T_1^{(6)'}$ are non-congruent tilings up to rigid motions. Similarly, $T_3^{(6)}$ and $T_4^{(6)}$ are not mirror symmetric. Thus $T_3^{(6)}$ and $T_4^{(6)}$ each give rise to two non-congruent tilings in $\mathbb{X}_{\sigma_6}$ invariant under threefold rotation.

Consider the list of vertex stars given in Fig. 17. Observe that among them, $\mathcal{V}_{6,3}$, $\mathcal{V}_{6,4}$ and $\mathcal{V}_{7,2}$ and its reflected copy $\mathcal{V}_{7,3}$ have rotational symmetry. From theorem 12, $\mathcal{V}_{6,3}$ and $\mathcal{V}_{6,4}$ are seeds for tilings in $\mathbb{X}_{\sigma_6}$ invariant under twofold rotation. Now, as indicated by the blue arrows in Fig. 17, the centre of $\sigma_6(\mathcal{V}_{7,2})$ is $\mathcal{V}_{7,3}$ and the centre of $\sigma_6(\mathcal{V}_{7,3})$ is $\mathcal{V}_{7,2}$. Thus, $(\sigma_6^{2k}(\mathcal{V}_{7,2}))_{k\in\mathbb{N}}$ and $(\sigma_6^{2k}(\mathcal{V}_{7,3}))_{k\in\mathbb{N}}$ yield two additional tilings invariant under twofold rotation in $\mathbb{X}_{\sigma_6}$.

The edge types that are invariant under twofold rotation are shown in Fig. 21. It can be checked that the central patch of $\sigma_6^k(E_i)$, $i = 1, 2, \ldots, 8$, is either an equivalent copy of E_1 or E_2 for all i and $k \geq 2$. Thus, we consider E_1 and E_2 as the only edge types that can be seeds for tilings invariant under twofold rotation. As illustrated in Fig. 22, E_1 and E_2 are the central patches of $\sigma_6(E_2)$ and $\sigma_6(E_1)$, respectively. As above, $(\sigma_6^{2k}(E_1))_{k\in\mathbb{N}}$ and $(\sigma_6^{2k}(E_2))_{k\in\mathbb{N}}$ converge to two tilings in $\mathbb{X}_{\sigma_6}$. The vertex stars $\mathcal{V}_{6,3}$ and $\mathcal{V}_{6,4}$ and edge types E_1 and E_2 are not mirror symmetric, so their reflected copies can also serve as seeds for tilings invariant under twofold rotation. Therefore, there are ten non-congruent tilings in $\mathbb{X}_{\sigma_6}$ invariant under twofold rotation. □

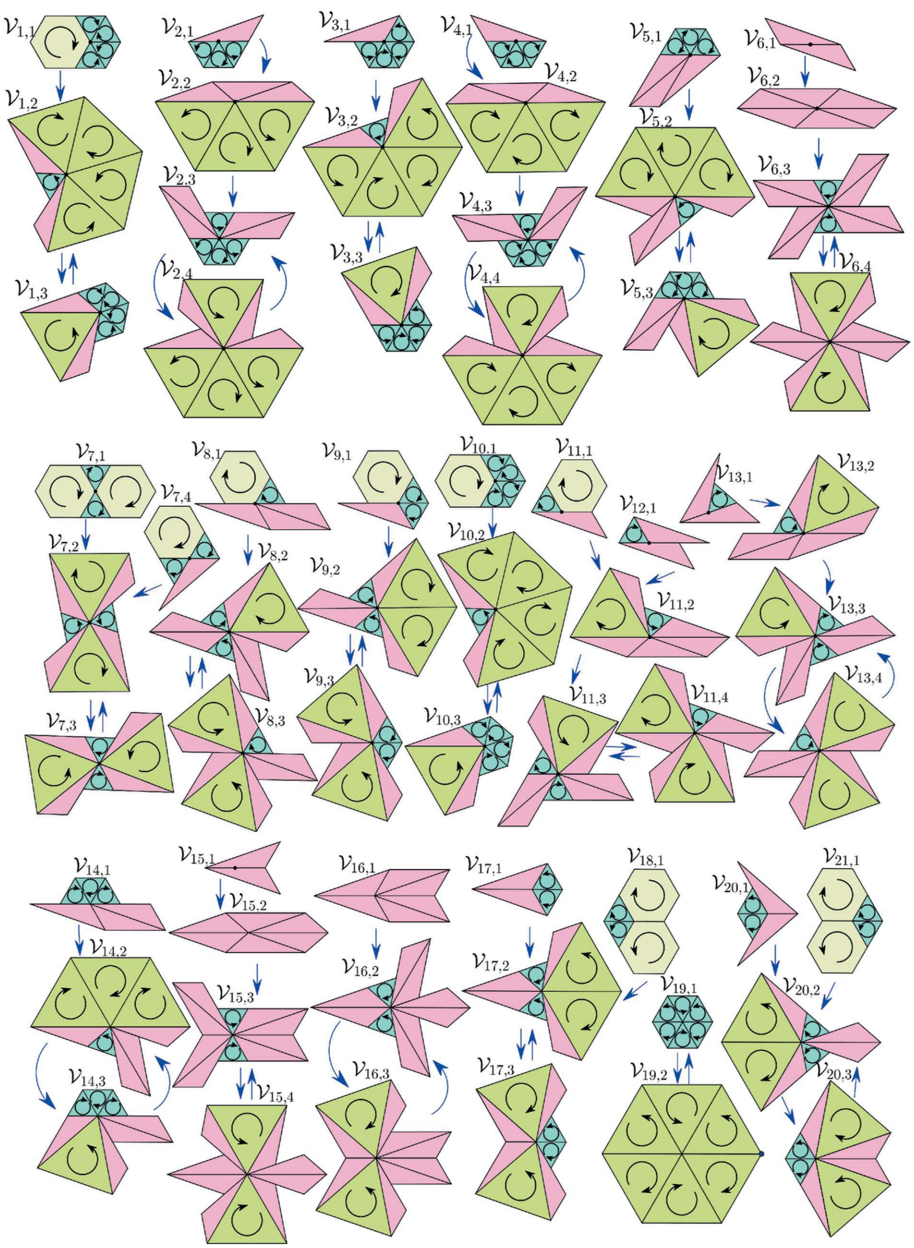

Figure 17
The list of non-equivalent vertex stars in $\mathcal{T} \in \mathbb{X}_{\sigma_6}$. Blue arrows indicate the action of σ_6 as illustrated in Fig. 18.

5. Conclusion

In this article we have presented primitive substitutions σ_6 and σ_7 which generate substitution tilings with DTO and which are invariant under sixfold and sevenfold rotations, respectively. We have also identified properties of the tilings in $\mathbb{X}_{\sigma_n}$, $n = 6, 7$, such as FLC, repetitivity and aperiodicity.

The algorithm described in this work can be used to obtain other tilings invariant under n-fold rotation ($n = 3, 4, 5, 6, 8$) given by Frettlöh *et al.* (2017) and this can also be adopted to construct higher-ordered rotation-invariant tilings. Starting with a regular n-gon $T_1^{(n)}$ and a scalene triangle $T_2^{(n)}$ with irrational angle α_n, the process may be iterated to obtain a substitution tiling $\mathcal{T}_n$ with DTO that is invariant under n-fold rotation. The prototile $T_1^{(n)}$ serves as a seed for $\mathcal{T}_n$, which is a fixed point of $\mathfrak{R}_{\alpha_n}\sigma_n$. There is a pattern that emerges for dissection of $\lambda_n T_1^{(n)}$ into one copy of $\lambda_n T_1^{(n)}$, n copies of $T_2^{(n)}$ and parallelograms (Fig. 4), and $\lambda_n T_2^{(n)}$ into copies of $T_2^{(n)}$ and other triangle prototiles. However, the number of prototiles is expected to be large for some values of

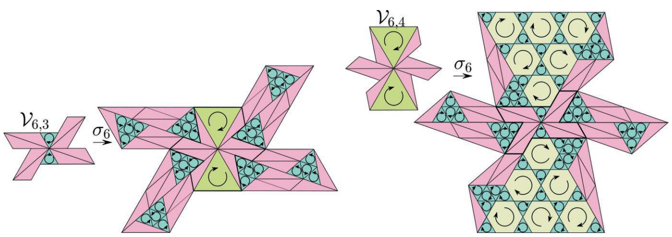

Figure 18
Vertex stars in $\mathcal{T} \in \mathbb{X}_{\sigma_6}$ with rotational symmetry and their images under σ_6.

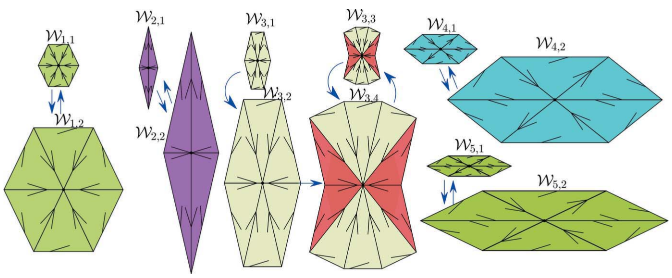

Figure 19
Some non-equivalent vertex stars in $\mathcal{T} \in \mathbb{X}_{\sigma_7}$ that are invariant under twofold rotation. Blue arrows indicate the action of σ_7.

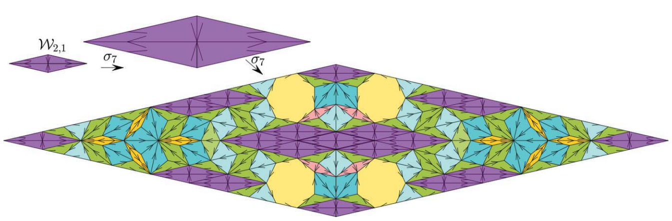

Figure 20
$\sigma_7^2(\mathcal{W}_{2,1})$ contains $\mathcal{W}_{2,1}$ in its centre.

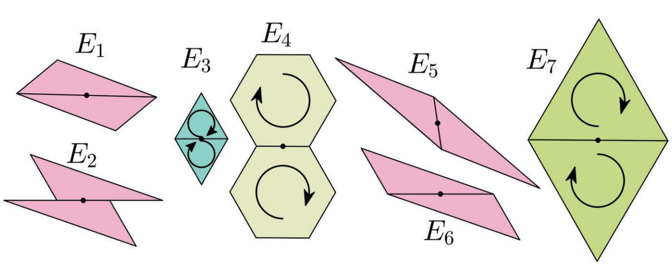

Figure 21
Edge types of $\mathcal{T} \in \mathbb{X}_{\sigma_6}$ with rotational symmetry.

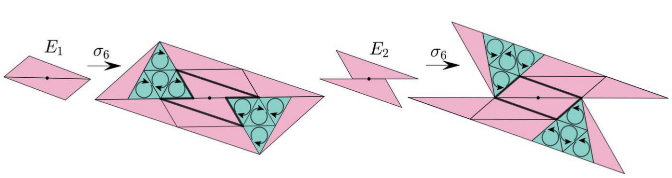

Figure 22
Edge types E_1 and E_2 and their images under σ_6.

n; more so if the tilings are constructed to satisfy other properties.

Another aspect discussed in this study is the notion of symmetry order of the hull of a substitution tiling. The method employed in determining the symmetry order entailed looking at a patch (either a prototile, vertex star or edge type) that is invariant under r-fold rotation that can serve as a seed for an r-fold rotation-invariant tiling in the hull.

Interestingly, the derived results in this work have implications in the context of dynamical properties of the hull. For instance, Frettlöh & Richard (2014) state that the repetitivity of $\mathcal{T} \in \mathbb{X}_{\sigma_n}, n \in \{6, 7\}$, implies the minimality of the dynamical system $(\mathbb{X}_{\sigma_n}, G)$, where G is the group of translations or direct Euclidean motions. Moreover, proposition 2.12 of Frettlöh & Richard (2014) states that $\mathcal{T}$ is linearly repetitive, due to the primitivity of σ_n and the FLC property of $\mathcal{T} \in \mathbb{X}_{\sigma_n}$. In addition, the linear repetitivity of $\mathcal{T} \in \mathbb{X}_{\sigma_n}$ implies that $(\mathbb{X}_{\sigma_n}, G)$ is uniquely ergodic (Lagarias & Pleasants, 2003; Frettlöh & Richard, 2014). It would be a good idea to explore the dynamical properties of the respective hulls of the constructed tilings presented in this work.

In relation to the study of cohomology groups, results from Barge *et al.* (2010) assert that the occurrence of tilings invariant under s-fold rotation in the hull of a substitution implies that the second cohomology group of the hull has a torsion subgroup. For example, for $\mathbb{X}_{\sigma_6}$, the ten tilings in $\mathbb{X}_{\sigma_6}$ that are invariant under twofold rotation contribute a torsion subgroup $\mathbb{Z}_2^{10-1} = \mathbb{Z}_2^9$ to the second cohomology group of $\mathbb{X}_{\sigma_6}$. Hence it becomes interesting to determine the number of tilings in the hull of a given substitution that are invariant under s-fold rotation up to direct Euclidean motions.

Funding information

The following funding is acknowledged: Accelerated Science and Technology Human Resource Development Program (ASTHRDP) of the Department of Science and Technology (DOST) (scholarship to April Lynne D. Say-awen); German Academic Exchange Service (DAAD) (grant to Ma. Louise Antonette N. De Las Peñas).

References

Baake, M., Frettlöh, D. & Grimm, U. (2007*a*). *J. Geom. Phys.* **57**, 1331–1343.
Baake, M., Frettlöh, D. & Grimm, U. (2007*b*). *Philos. Mag.* **87**, 2831–2838.
Baake, M. & Grimm, U. (2013). *Aperiodic Order: A Mathematical Invitation*, Vol. 1. Cambridge University Press.
Barge, M., Diamond, B., Hunton, J. & Sadun, L. (2010). *Ergod. Th. Dyn. Syst.* **30**, 1607–1627.
Frank, N. P., Webster, S. B. & Whittaker, M. F. (2016). *J. Fractal Geom.* **3**, 265–317.
Frettlöh, D. (2008). *Eur. J. Combin.* **29**, 1881–1893.
Frettlöh, D. (2017). *Aperiodic Order: Crystallography and Almost Periodicity: More Inflation Tilings*, Vol. 2, edited by M. Baake & U. Grimm. Cambridge University Press.
Frettlöh, D. & Richard, C. (2014). *Discrete Contin. Dyn. Syst.* **34**, 531–556.

Frettlöh, D., Say-awen, A. L. D. & De Las Peñas, M. L. A. N. (2017). *Indag. Math.* **28**, 121–131.
Frettlöh, D., Whitehead, B. & Whittaker, M. (2014). *J. Aust. Math. Soc.* **97**, 162–179.
Grimm, U. & Deng, X. (2011). *J. Phys. Conf. Ser.* **284**, 012032.
Grünbaum, B. & Shephard, G. C. (1986). *Tilings and Patterns*. New York: W. H. Freeman and Company.
Kari, J. & Rissanen, M. (2016). *Discrete Comput. Geom.* **55**, 972–996.
Lagarias, J. C. & Pleasants, P. A. B. (2003). *Ergod. Th. Dyn. Syst.* **23**, 831–867.
Maloney, G. R. (2015). *Discrete Math. Theor. Comput. Sci.* **17**, 397–414.
Moody, R. V., Postnikoff, D. & Strungaru, N. (2006). *Ann. H. Poincaré*, **7**, 711–730.
Penrose, R. (1978). *Eureka*, **39**, 16–32.
Radin, C. (1994). *Ann. Math.* **139**, 661–702.
Radin, C. (1995). *Geom. Dedicata*, **55**, 257–264.
Savinien, J. & Frettlöh, D. (2013). Personal communication.
Say-awen, A. L. D. (2016). PhD thesis, Ateneo de Manila University, Loyola Heights, Quezon City, Philippines.